Energy Proceedings
Vol 62, 2026
ISSN 2004-2965

Experimental Study of Elastic Lost Circulation Materials for Dynamic Fracture Losses in CO_2 Storage Well Drilling

Han Hu[1], Yongcun Feng[2*],Ruixue Wang[3]

1 College of Petroleum Engineering, China University of Petroleum, Beijing, China

2 College of safety and Ocean Engineering, China University of Petroleum, Beijing, China

3 Sinopec North China Petroleum Bureau, Zhengzhou, Henan 450006, China

(Corresponding Author: yfeng@cup.edu.cn)

ABSTRACT

During drilling CO_2 storage and monitoring wells, maintaining fracture stability is critical for preserving future injectivity and caprock sealing efficiency. Fluctuating bottom-hole pressure can induce cyclic deformation of natural fractures by transient drilling operations. This dynamic behavior destabilizes the plugging layer, making conventional lost circulation materials (LCMs) inadequate for sustained plugging performance. To address this problem, this study experimentally investigates the plugging behavior and formulation design criteria of three elastic LCMs including rubber particles, elastic graphite, and elastic mesh material under both static and dynamically deforming fracture conditions. The effects of particle size distribution, material proportion, pressure-bearing capacity, resealing behavior, and fracture-width adaptability were quantified. Experimental results demonstrate that appropriate coordination among three elastic materials enables controlled migration of the bridging zone within the fracture and significantly increases the fracture reopening pressure. When the particle size distribution of each elastic material is within its respective optimal range and the composite mass ratio satisfies filling: auxiliary bridging: secondary auxiliary bridging = 4:2:1, the optimized ternary formulation preferentially forms a tight, low-permeability, and extraction-resistant plugging layer. The plugging layer exhibits both higher reopen pressure and strong adaptability to dynamic changes in fracture width. These findings provide a scientific theoretical basis for mitigating drilling-induced losses and supporting wellbore stability management in CO_2 storage well drilling.

Keywords: CCS, Pressure Fluctuation, Plugging, Fracture Deformation

NONMENCLATURE

Abbreviations	
LCM	Lost Circulation Material
CCS	Carbon Dioxide Capture and Storage
PSD	Particle Size Distribution

1. INTRODUCTION

Wellbore stability is a critical criterion for the long-term safety and effectiveness of carbon dioxide capture and storage (CCS) projects. Extensive research has focused on stability evaluation during the injection and storage stages. As the starting point of wellbore construction, the drilling process also has a decisive impact on wellbore injectivity and caprock sealing integrity (Takase et al.,2010, Vialle et al.,2016). During the drilling of injection and monitoring wells, encountering natural fractures or weak planes increases the risk of loss circulation. If plugging measures fail, the drilling schedule will be prolonged, hidden risks are also introduced for subsequent CO_2 injection and storage operations, including wellbore failure and CO_2 leakage (Nordbotten, 2005, Oldenburg, 2007).

one critical challenge is the fluctuation of bottom-hole pressure during transient operations. Operations such as swab and surge during tripping, the start-up and shutdown of pump systems, and the switching of drilling fluid circulation can all induce pressure fluctuations. These abnormal fluctuations drive the opening and closing of stress-sensitive fractures which called “breathing effect” (Gao et al.,2020, Ma et al., 2024). The breathing effect leads to the instability of the sealing zone and repeated leakage (Xu et al., 2017, Gao et al.,2025). Compared to static conditions, sealing under dynamic fracture deformation is more demanding. It not only requires materials to achieve effective bridging and filling but also demands that the sealing zone maintain

This is a paper for the 17th International Conference on Applied Energy (ICAE2025), December 8-12, 2025, Bangkok, Thailand.

pressure-bearing stability under varying fracture widths and cyclic loading (Kumar et al., 2011; Gao et al., 2020). However, most existing studies are confined to static fracture experiments or single-cycle pressure-bearing evaluations. There is a lack of understanding regarding the dynamic mechanisms of plugging layers under pressure fluctuation conditions, as well as a shortage of design and evaluation methods.

Elastic LCMs have been increasingly applied in fractured formations in recent years. Elastic LCM systems exhibit deformability and elastic recovery, which assists rigid bridging particles maintain contact and pressure-bearing capacity under varying fracture widths. However, elastic materials also have significant limitations. The effective size of elastic particles under pressure and their bridging threshold are difficult to quantitatively calibrate (Vickers et al., 2006, Whitfill, 2008). High-concentration formulations tend to accumulate at the fracture entrance and the formed plugging layer is prone to localized instability due to drilling fluid erosion. In contrast, low-concentration formulations struggle to rapidly form an effective plugging layer (Alberty & McLean, 2004; Salehi et al., 2016). To address these challenges, this study focuses on dynamic fracture scenarios during CCS well drilling, where plugging performance must be maintained under fluctuating fracture widths. An experimental evaluation and optimization method is proposed for elastic LCM systems, aiming to balance bridging stability, sealing strength, and adaptability to dynamic fracture deformation.

2. THEORETICAL BASIS AND FORMULATION CRITERIA

The essence of fracture-based lost circulation control lies in establishing a reliable mapping between material particle size, plugging structure, and resulting performance. Therefore, the rational design of particle size distribution (PSD) is a prerequisite for constructing an effective bridging layer.

Abrams (1977) suggests in classic “1/3 rule” that the particle diameter for bridging should be no less than one-third of the target pore throat size, and also provides a minimum effective concentration threshold. Building upon this, subsequent studies have proposed more refined particle size and concentration combinations for bridging and packing (Luo et al.,1992; Li et al.,2023)

To overcome the limitations of unimodal distributions, criteria based on D50/D90 and multimodal PSD have been introduced as effective design windows (Smith et al., 1996, Hand et al., 1998). Extensive experimental studies have demonstrated that when D50 and D90 maintain stable proportional relationships with fracture aperture, enhanced plugging efficiency can be achieved across varying widths (Wang et al., 2019). In this context, D90 primarily governs the bridging threshold, while D50 reflects the skeletal framework scale. Considering both in tandem allows effective plugging over a wider aperture range. Complementary to this, ideal packing or multi-modal packing theories advocate using multiple particle size groups with tailored volume fractions to increase packing density and reduce permeability of the plugging layer (Alberty & McLean, 2001).

On the other hand, wellbore strengthening strategy, often described by the Stress Cage Mechanism, aims to relocate the primary bridging zone from the fracture entrance deeper into the fracture body (Feng & Gray, 2018). This approach enhances the fracture breakdown pressure and raises the refracture threshold pressure, thereby improving the overall integrity margin. However, its effectiveness is highly sensitive to both particle size distribution and concentration. Excessive entrance accumulation can lead to seal failure caused by drilling fluid erosion, compromising the long-term plugging stability.

Therefore, a clear evaluation method was established based on previous theories. First, the ratio between particle size and fracture width is used to define the functional roles of each type of elastic material, determining their representative size ranges and expected bridging positions. Next, based on the multimodal PSD theory, the volume fractions of large, medium, and small particles are selected. Finally, the formulations are validated and fine-tuned under dynamic loading conditions.

3. EXPERIMENTAL APPARATUS AND METHODS

The PPA plugging device was first used to optimize the formulation of three elastic materials, followed by evaluation under dynamic conditions with the DTDL dynamic-fracture plugging device.

3.1 PPA Plugging Device

The PPA high-temperature and high-pressure permeability plugging device is designed to simulate formation conditions and evaluate the fracture-plugging performance of LCM formulations. It supports maximum operating conditions of 35 MPa and 260°C, with a sample capacity of up to 275 mL per test.

Unlike conventional PPA setups that use cross-stitch or flat, this system introduces a wedge-shaped fracture module. The module is 5 mm long and tapers from 2 mm at the inlet to 1 mm at the outlet. It consists of two detachable plates, replicating realistic fracture geometry and allowing clear inspection of the sealed fracture after experiment.

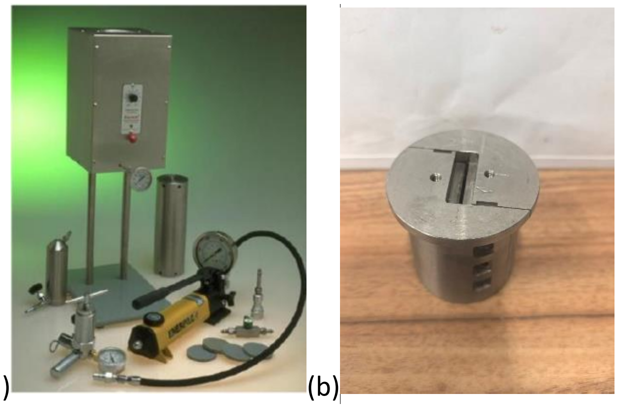
(a) (b)

Fig. 1 (a)PPA high-temperature and high-pressure permeability *plugging device (b)Fracture Module*

3.2 DTDL Dynamic Fracture Plugging Device

The DTDL plugging device is designed to evaluate the impact of pressure transients and fracture-width deformation on plugging layers. The fracture width is controlled by upper and lower slot plates. By altering the geometry of the fracture plates, the setup can be configured to generate parallel-plate, wedge-shaped, and curved fractures. The upper plate is connected to a hydraulic pump with two floating pistons. Variations in drilling fluid pressure drive movement of the upper plate, dynamically adjusting the fracture width in real time. These width changes are accurately recorded using a micrometer. The device supports maximum operating conditions of 20 MPa and 150°C, with a sample capacity of up to 1 liter per test.

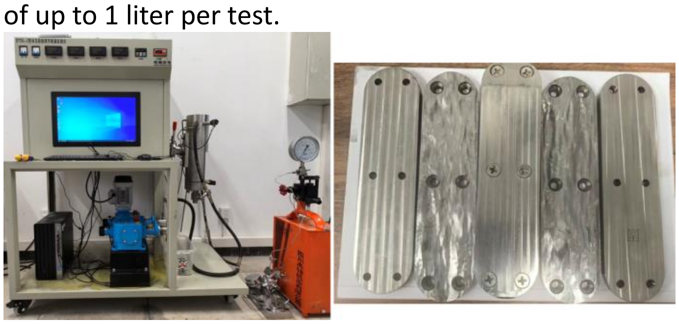

Fig. 2 DTDL Dynamic Fracture Plugging Device

3.3 Experimental Methods

The base mud formulation in this study consisted of distilled water, 8% bentonite, 0.2% sodium carbonate (Na_2CO_3), and 0.5% PAC-141. Table 1 summarizes the properties of the base mud.

Table 1.Paramerers of Fundamental Slurry

Parameter	*Apparent Viscosity (mPa.s)*	*Plastic Viscosity (mPa.s)*	*Shear Stress (Pa)*	*Density (g/cm^3)*
Performance	38.5	27	11.5	1.04

According to literature review, conventional plugging materials use walnut shells as bridging particles to form the seal layer skeleton. Sawdust and mica are used as filling materials to pack the voids between bridging particles, creating a dense plugging layer. Recycled tire rubber, elastic graphite, and elastic mesh material "poreseal-5" were chosen as elastic materials shown in Fig. 3. When wellbore pressure increases and fracture width expands, these elastic particles deform to fill the enlarged voids, enhancing fracture re-opening pressure and the pressure-bearing capacity of plugging layer. Han (2025) used a mixing ratio of 4:3.6:2.4 for conventional plugging material which was adopted in this experimental study.

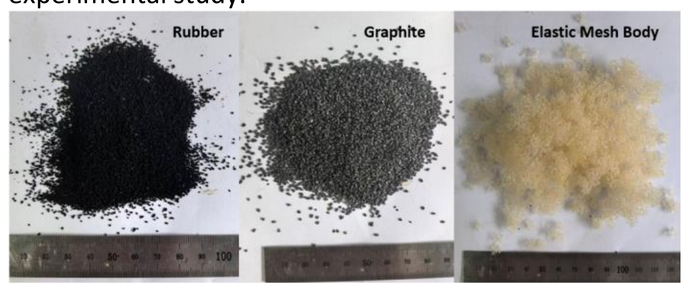

Fig. 3 Elastic LCMs Sample

For designing fracture plugging formulations, evaluating the LCM particle size is essential. The D10, D50, and D90 values of elastic particles of different mesh sizes were measured using sieve analysis and laser particle size analysis. Table 2 presents the particle size distribution results of the elastic particles used in this study. To evaluate LCM performance, five key indicators were selected including fluid loss, pressure-bearing capacity, plugging layer location, deformation tolerance, and resealing time.

Table.2 Elastic particle size evaluation results

Size(mesh)	D10	D50	D90
6-10	1400-1700	1700-2360	2360-3350
10-20	830-880	1180-1400	1400-1700
14-20	700-830	1000-1180	1000-1180
20-32	600-646	646-700	646-700
32-60	250-260	325-380	380-425
40-60	<250	270-325	325-380

4. EXPERIMENTAL RESULTS AND ANALYSIS A

4.1 Individual Performance of Three Elastic Materials

Two concentrations 11% and 13% were tested at 10 MPa to evaluate the pressure-bearing capacity of the plugging layer. As shown in Fig. 4, fluid loss decreased with smaller rubber particle sizes. Elastic graphite, however, exhibited the opposite trend. Therefore, a higher proportion of small rubber particles and large graphite particles is required, when testing the hypothesis that multi-size particle composites are more effective than single-size ranges.

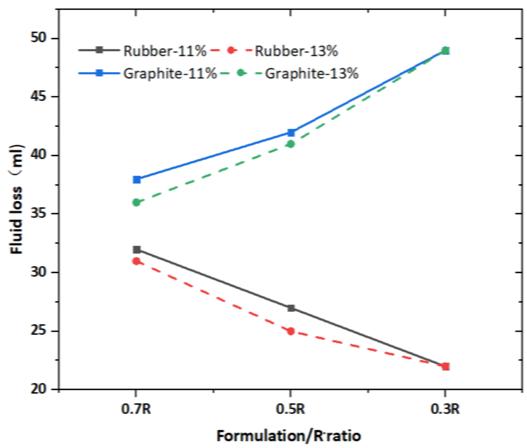

Fig. 4 Comparison of fluid loss with different R ratio

As shown in Figures 5, compared with the single-size bridging particle, multi-size collaboration alters the structure of the plugging zone, enhancing its density and strength. Rubber particles utilize their compressibility and rebound properties to achieve filling between bridging skeletons, reducing the permeability of the plugging layer. Elastic graphite particles provide auxiliary bridging support, helping walnut particles form a stable framework within the fracture, thereby influencing the plugging layer's pressure-bearing capability and re-fracturing resistance.

However, over-reliance on a specific particle size can compromise stability. Excessive fine rubber particles may accumulate at the fracture inlet, leading to slippage and instability of plugging layer during dynamic fracture opening-closing cycles. Conversely, excessive large graphite particles may leave voids in the bridging skeleton, resulting in failure. Therefore, the selected particle size distributions were optimized as large:medium:small = 1:5:4 for rubber and 6:3:1 for graphite.

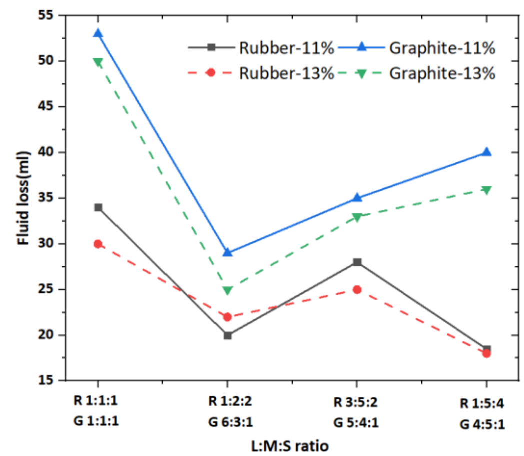

Fig. 5 Comparison of fluid loss with different

Figure 6 shows that elastic mesh materials promote the transition from localized accumulation to a continuously pressure-bearing plugging layer across the fracture which improve pressure bearing limits of plugging zone. All experiments described above confirm the complementary roles of the three elastic materials in enhancing pressure-bearing capacity, reducing the permeability of the plugging layer, and increasing the effective plugging length, thereby providing a reliable basis for the subsequent design and optimization of composite formulations.

Fig.6 Bridging condition with Elastic Mesh Material

4.2 Influence of Elastic Material Concentration

While the fracture aperture dynamically increases, the interparticle voids within the plugging layer enlarge correspondingly. However, the bridging skeleton does not exhibit significant slippage before plugging layer fails. Therefore, the concentration of filling particles needs to be relatively higher than the bridging-assist particles. To validate this hypothesis, systematic tests were conducted on the concentrations of composite formulation materials, focusing on pressure-bearing capacity, fluid loss, and bridging time (Fig. 9).

Experimental results, shown in Table 3, indicate that the concentration distribution among the three materials should follow the principle of maintaining the highest proportion of rubber, graphite in the middle, and the lowest for mesh material. While increasing the rubber content can further reduce fluid loss, it significantly raises the risk of particle accumulation near the fracture entrance. Excessive graphite content can overly compromise the structural stability of the plugging layer, and increase its permeability. An overabundance of mesh material restricts the mobility of particles relative to each other and to the surrounding fluid, causing fine particles to accumulate near the entrance. An insufficient amount of mesh material leads to discontinuities in plugging layer compactness and increases the risk of localized instability. Compared to binary systems, ternary formulations demonstrate higher pressure-bearing capacity and lower fluid loss under the same total concentration. The composition R:G:M = 3:2:1 is identified as the optimal formulation within the current fracture width and concentration window, as it balances bridging, compactness, and tolerance to fracture width variation. The R:G:M = 2:3:1 formulation is considered additional supplement. These two candidate formulations will be further verified using the DTDL experimental system under dynamic fracture width and pressure cycling conditions, with minor adjustments to be made accordingly.

Table 3 *Elastic material plugging performance results*

No.	Gross Content of Elastic Material	Pressure(MPa)	Fluid Loss Amount (ml)	Pressurization Cycles
1	R:G=1:1	9	36	9
2	R:G=2:1	10	28	8
3	R:G=1:2	7	42	10
4	R:M=3:1	10	25	7
5	G:M=3:1	6	31	12
6	R:G:M=1:1:1	8	22	9
7	R:G:M=2:3:1	9	18	9
8	R:G:M=3:2:1	10	14	7

4.3 Formulation Validation and Adjustment

Based on all experimental results above, candidate formulations were further evaluated under dynamic conditions by re-establishing the plugging layer at the same fracture width. Experimental results, shown in Table 4, reveal that as rubber primarily serves as a filling particle, slightly increasing its proportion does not produce the adverse effects for plugging performance. The graphite dominant ternary formulation exhibited pressure-bearing capacity and tolerance to deformation reduction during the dynamic condition. However, it showed the fastest re-bridging response after failure, indicating that elastic graphite contributes to rapid re-establishment of bridging structures. Ternary formulations with higher rubber content than graphite exhibited higher pressure-bearing capacity and lower fluid loss during cyclic loading. They also demonstrated greater tolerance to fracture width fluctuations, outperforming the binary formulations in plugging stability. The concentration of mesh material was found to be more sensitive under dynamic conditions. Excessive mesh materials led to severe plugging at the fracture entrance, making it difficult for the bridging zone to migrate into the fracture and extend along its length. Therefore, the optimal compositional window under dynamic fracture conditions should satisfy the constraint that the rubber content is greater than the graphite content, while the mesh content remains at its minimum effective dosage. Accordingly, R:G:M ratios of 4:2:1 or 3:2:1 are identified as more robust baseline formulations for dynamic applications.

(a) Binary formulation bridging condition

(b) Ternary formulation bridging condition

Fig. 7 Comparison of bridging conditions with different formulations

Table 4 Elastic material plugging performance results

No.	Gross Content of Elastic Material	Pressure(MPa)	Fluid Loss Amount (ml)	Fracture Deformation (mm)	Re-sealing Speed Rank
1	R:M=3:1	6	122	0.604	4
2	G:M=3:1	4	Unplugged	Unplugged	--
3	R:G:M=2:3:1	5.5	143	0.405	1
4	R:G:M=3:2:1	6	111	0.786	2
5	R:G:M=4:2:1	6	92	0.822	3

5. CONCLUSIONS

1. In the optimization of elastic particle formulations, rubber particles with medium-to-small sizes are preferred for reducing the permeability of the plugging layer. Graphite particles with medium-to-large sizes serve to assist rigid particles in effective bridging. When used at the minimum effective dosage, elastic mesh materials contribute to extending the plugging length and improving strength continuity of the plugging structure.
2. Ternary formulations outperform binary ones in terms of pressure-bearing capacity, loss reduction, and cyclic stability. The formulation with a representative ratio of R:G:M = 4:2:1 exhibits the best comprehensive performance. Under pressure cycling and fracture opening increments, the optimized formula maintains stable bridging positions and tolerates up to 41.1% fracture width increase without structural failure.
3. An effective optimization strategy was established. In this strategy, rubber particles enhance the compactness of the sealing structure, graphite controls the bridging location and contributes to resealing performance, while mesh materials improve the continuity and integrity of the plugging layer. Formulations optimized in this sequence have demonstrated the ability to effectively seal fractures, form dense internal plugging structures, prevent the development of early leakage pathways, and preserve the long-term injectivity of the well.

ACKNOWLEDGEMENT

This research was funded by National Natural Science Foundation of China (grant number. 52374009)

REFERENCE

[1]Abrams, A. (1977). Mud design to minimize rock impairment due to particle invasion. Journal of Petroleum Technology, 29(5), 586–592.

[2]Alberty, M., & McLean, M. (2001). Fracture gradients in depleted reservoirs—Drilling wells in late reservoir life. Paper presented at the SPE/IADC Drilling Conference.

[3] Alberty, M. W., & McLean, M. R. (2004). A physical model for stress cages. In *SPE Annual Technical Conference and Exhibition, Houston, Texas, USA.*

[4]Feng, Yongcun , and K. E. Gray. Modeling Lost Circulation Through Drilling-Induced Fractures. SPE J. 23 (2018): 205–223.

[5]Gao, R., Li, J., Liu, G., Yang, H., Luo, K., Zhai, W., & Zhang, R. (2020). Experimental study on typical characteristics of borehole breathing under different pressure and rock type conditions. *Journal of Natural Gas Science and Engineering*, *77*, 103241.

[6]Gao, R., Cui, Y., Wang, G., Zhao, F., & Ding, Y. (2025). Dynamic response mechanism of borehole breathing in fractured formation. In *International Conference on Computational & Experimental Engineering and Sciences*. Springer, Cham.

[7]Hands, N., Kowbel, K., Maikranz, S., & Nouris, R. (1998). Drill-in fluid reduces formation damage, increases production rates. Oil & Gas Journal, 96(28).

[8]Hu, H., Feng, Y., Lai, C., Li, X., & Wang, G. (2025, June). Mechanism of dynamic deformation in stress-sensitive fractures and adaptive plugging formulation development. In *ARMA US Rock Mechanics /Geomechanics Symposium* (pp. ARMA-2025). ARMA.

[9]Kumar, A., Savari, S., Whitfill, D., & Jamison, D. (2011, April). Application of fiber laden pill for controlling lost circulation in natural fractures. In *AADE national technical conference and exhibition, Houston, Texas, USA* (pp. 12-14).

[10]Li, B., Feng, Y., Ma, C., Li, S., Lai, C., Zhang, S., & Su, F. (2023, June). Particle size optimization of lost circulation materials: a comprehensive experimental study. In *ARMA US Rock Mechanics/Geomechanics Symposium*. ARMA.

[11]Luo, X., & Luo, P. (1992). Protecting oil reservoir with temporary shielding method. *Drilling Fluid & Completion Fluid*, *9*(2), 19.

[12]Ma, C., Feng, Y., Dou, Y., Chu, M., Zhao, K., & Deng, J. (2024). Experimental study on the design method of lost circulation materials for induced fractures. Geoenergy Science and Engineering, 240, 213086.
[13]Nordbotten, J. M., Celia, M. A., & Bachu, S. (2005). Injection and storage of CO_2 in deep saline aquifers: Analytical solution for CO_2 plume evolution during injection. Transport in Porous Media, 58(3), 339–360.
[14]Oldenburg, C. M. (2007). Joule–Thomson cooling due to CO_2 injection into natural gas reservoirs. Energy Conversion and Management, 48(6), 1808–1815.
[15]Smith, P. S., Browne, S. V., Heinz, T. J., & Wise, W. V. (1996, October). Drilling fluid design to prevent formation damage in high permeability quartz arenite sandstones. In *SPE Annual Technical Conference and Exhibition*. SPE.
[16]Salih, A., & Hussein, H. A. A. (2022). Artificial intelligent models for detection and prediction of lost circulation events: A review. Iraqi Journal of Chemical and Petroleum Engineering, 23(4), 81–90.
[17]Takase, K., Barhate, Y., & Hashimoto, H. (2010). Cement-sheath wellbore integrity for injection and storage wells. In *SPE Oil and Gas India Conference and Exhibition. Society of Petroleum Engineers, Mumbai, India*.
[18]Vialle, S., Druhan, J. L., & Maher, K. (2016). Multi-phase flow simulation of CO_2 leakage through a fractured caprock in response to mitigation strategies. International Journal of Greenhouse Gas Control, 44, 11–25.
[19]Wang, G., Huang, Y., & Xu, S. (2019). Laboratory investigation of the selection criteria for the particle size distribution of granular lost circulation material in naturally fractured reservoirs. Journal of Natural Gas Science and Engineering, 71, 103000.
[20]Xu, C., Kang, Y., You, L., & You, Z. (2017). Lost-circulation control for formation-damage prevention in naturally fractured reservoir: Mathematical model and experimental study. SPE Journal, 22(5), 1654–1670.